Mimicking the First Step of RNA Splicing: An Artificial DNA Enzyme Can Synthesize Branched RNA Using an Oligonucleotide Leaving Group as a 5′-Exon Analogue†

Rebecca L. Coppins and Scott K. Silverman*

Department of Chemistry, University of Illinois at Urbana-Champaign, 600 South Mathews Avenue, Urbana, Illinois 61801

Received April 19, 2005; Revised Manuscript Received August 10, 2005

ABSTRACT: The 7S11 deoxyribozyme synthesizes 2′,5′-branched RNA by mediating the nucleophilic attack of an internal 2′-hydroxyl group of one RNA substrate into the 5′-triphosphate of a second RNA substrate, with pyrophosphate as the leaving group. Here we comprehensively examined the role of the leaving group in the 7S11-catalyzed reaction by altering the 5′-phosphorylation state and the length of the second RNA substrate. When the leaving group is the less stabilized phosphate or hydroxide anion as provided by a 5′-diphosphate or 5′-monophosphate, the same 2′,5′-branched product is formed as when pyrophosphate is the leaving group, but with an ∼50- or ∼1000-fold lower rate (Brønsted $\beta_{LG} = -0.40$). When the 5′-end of the RNA substrate that bears the leaving group is longer by one or more nucleotides, either the new 5′-terminal α-phosphate or the original α-phosphate can be attacked by the branch-site 2′-hydroxyl group; in the latter case, the leaving group is an oligonucleotide. The choice between these α-phosphate reaction sites is determined by the subtle balance between the length of the single-stranded 5′-extension and the stability of the leaving group. Because the branch-site adenosine is a bulged nucleotide flanked by Watson−Crick duplex regions, we earlier concluded that 7S11 structurally mimics the first step of natural RNA splicing. The observation of 7S11-catalyzed branch formation with an oligonucleotide leaving group strengthens this resemblance to natural RNA splicing, with the oligonucleotide playing the role of the 5′-exon in the first step. These findings reinforce the notion that splicing-related catalysis can be achieved by artificial nucleic acid enzymes that are much smaller than the spliceosome and group II introns.

Explorations of artificial ribozymes and deoxyribozymes have implications for the capabilities and limitations of nucleic acid catalysis. These efforts have conceptual importance in the context of the "RNA world" hypothesis, which postulates a primordial epoch when RNA performed both genetic and catalytic functions (*1*, *2*). Most if not all reactions catalyzed by natural ribozymes involve phosphodiester exchange or hydrolysis (*3*), and artificial nucleic acid enzymes that mediate similar reactions have been frequent experimental targets (*4*). Our laboratory's efforts with deoxyribozymes (*5*) have focused on RNA ligation (*6*−*19*). We recently used in vitro selection to identify 7S11, a DNA enzyme that structurally mimics the first step of RNA splicing by catalyzing the nucleophilic attack of a bulged adenosine 2′-hydroxyl group into a 5′-triphosphate, forming 2′,5′-branched RNA (Figure 1A) (*12*, *14*). However, the mimicry of RNA splicing by 7S11 is imperfect in this reaction because the leaving group is a poor 5′-exon analogue (i.e., not an oligonucleotide). Instead, the leaving group is pyrophosphate, which is much better in this role than an oligonucleotide.

Earlier, we tested one structural analogue of a 5′-triphosphate, the 5′-adenylated RNA substrate (5′-AppRNA)[1] (*20*), which was found to function well in 7S11-mediated RNA ligation (*12*, *14*). This demonstrated that 7S11 does not strictly demand a pyrophosphate leaving group, which in turn suggested that other leaving group modifications may also be tolerated. In the current study, we have investigated the precise substrate requirements for 7S11 branch formation by varying both the leaving group itself and its position with respect to the branch site nucleotide. When the substrate is changed from 5′-triphosphate to 5′-diphosphate or 5′-monophosphate, thereby altering the leaving group from pyrophosphate (PP_i) to the poorer leaving group phosphate (P_i) or hydroxide (HO^-), the rate of branch formation is reduced. Separately, extending the 5′-terminus of the substrate establishes a competition between two reaction sites for nucleophilic attack of the branch-site 2′-hydroxyl group (Figure 1B). These two sites are the α-phosphate at the 5′-terminus (which may be either 5′-triphosphate or 5′-mono-

† This research was supported by the Burroughs Wellcome Fund (New Investigator Award in the Basic Pharmacological Sciences), the March of Dimes Birth Defects Foundation (Research Grant 5-FY02-271), the National Institutes of Health (Grant GM-65966), the American Chemical Society Petroleum Research Fund (Grant 38803-G4), and the UIUC Department of Chemistry (all to S.K.S.). S.K.S. is the recipient of a fellowship from The David and Lucile Packard Foundation. R.L.C. is the recipient of a Sigma Xi Grant-in-Aid of Research.

* To whom correspondence should be addressed. Phone: (217) 244-4489. Fax: (217) 244-8024. E-mail: scott@scs.uiuc.edu.

[1] Abbreviations: 5′-AppRNA, 5′-adenylated RNA; PP_i, pyrophosphate; P_i, inorganic phosphate; PAGE, polyacrylamide gel electrophoresis; EDTA, ethylenediaminetetraacetic acid; T4 PNK, T4 polynucleotide kinase; CIP, calf intestinal phosphatase; CHES, 2-(*N*-cyclohexyl)aminoethanesulfonic acid; k_{obs}, observed rate constant; AMP, adenosine 5′-monophosphate; GMP, guanosine 5′-monophosphate.

10.1021/bi0507229 CCC: $30.25
Published on Web 09/21/2005

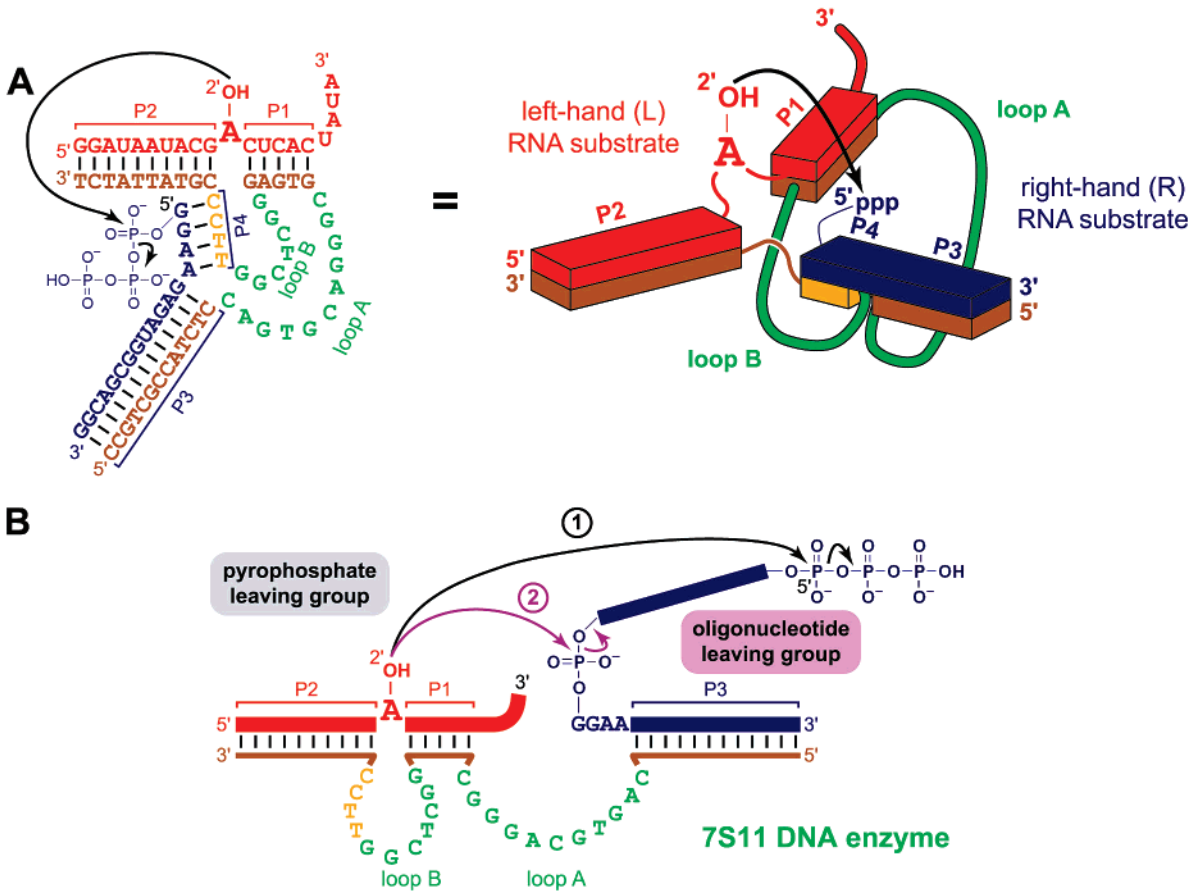

FIGURE 1: Formation of branched RNA by 7S11-catalyzed reaction of a branch-site adenosine 2′-hydroxyl group with a 5′-triphosphate (*12*). (A) Interactions between 7S11 and its RNA substrates. The existence of paired regions P1−P4 was inferred from extensive covariation data (*14*). Although the precise three-dimensional structure of 7S11 when complexed with its RNA substrates is unknown, the overall three-helix-junction structure is experimentally well-established (*14*). Red denotes the left-hand RNA substrate (L), and blue indicates the right-hand RNA substrate (R); the other colors represent the 7S11 DNA enzyme. (B) Competition between two α-phosphate reaction sites for nucleophilic attack of the branch-site 2′-hydroxyl group. The first reaction site is the α-phosphate of the 5′-terminal triphosphate, for which pyrophosphate is the leaving group (if the 5′-terminus is instead monophosphate, then the leaving group is hydroxide anion). The second site is the original internal α-phosphate, for which an oligonucleotide is the leaving group. For clarity, formation of P4 is not shown explicitly.

phosphate, with a leaving group of PP_i or HO^-) and the internal original α-phosphate (with an oligonucleotide as the leaving group). The balance between reactions at these two sites is controlled by the length of the 5′-extension and the stability of the leaving group. In general, our findings demonstrate that 7S11 has substantial plasticity for tolerating structural changes to its substrates. These findings for the 7S11 deoxyribozyme fit well with what is known about protein enzymes, which in a similar manner are often able to function with a range of substrates (see refs *21*−*24* for several recent examples).

Displacement of an unactivated oligonucleotide leaving group by the branch-site adenosine 2′-hydroxyl is mechanistically analogous to the 5′-exon serving as the leaving group during the first step of in vivo RNA splicing that is catalyzed by group II introns and the spliceosome. Therefore, our findings extend the structural parallel between 7S11 deoxyribozyme-catalyzed branched RNA formation and natural (e.g., spliceosomal) RNA splicing, strengthening the viewpoint that splicing-related catalysis can be performed by relatively small nucleic acid enzymes.

EXPERIMENTAL PROCEDURES

RNA and DNA Oligonucleotides. The 7S11 deoxyribozymes were prepared by solid-phase synthesis at IDT (Coralville, IA) and purified by denaturing PAGE with running buffer 1× TBE [89 mM Tris, 89 mM boric acid, and 2 mM EDTA (pH 8.3)] as described previously (*6*, *11*). The **0H** right-hand (R) RNA substrate was prepared by solid-phase synthesis at Dharmacon, Inc. (Lafayette, CO), and purified by denaturing PAGE. The **0D** and **0T**−**10T** R substrates as well as the left-hand (L) RNA substrate (which provides the 2′-hydroxyl nucleophile) were prepared by in vitro transcription using T7 RNA polymerase with an appropriate double-stranded DNA template (*25*). This procedure inherently provides a 5′-triphosphate electrophile on the **0T**−**10T** substrates. For the experiment whose results are depicted in Figure 6C, the internally radiolabeled pppR* was obtained by transcription in the presence of [α-^{32}P]CTP. The 5′-diphosphate of the **0D** substrate was obtained by inclusion of 10 mM GDP along with 0.5 mM GTP in the transcription solution (this leads to ∼5% **0T** in the sample of **0D**, which is without functional consequence; see the text). The **0M** substrate was prepared by monophosphorylation of **0H** with T4 polynucleotide kinase (PNK) and ATP. The L substrate was dephosphorylated with calf intestinal phosphatase (CIP) and then 5′-^{32}P-radiolabeled using [γ-^{32}P]ATP and PNK. For experiments in which L was 5′-phosphorylated without radiolabeling (Figures 3 and 6), unradiolabeled ATP and PNK were used. The **1H** and **2H** substrates were

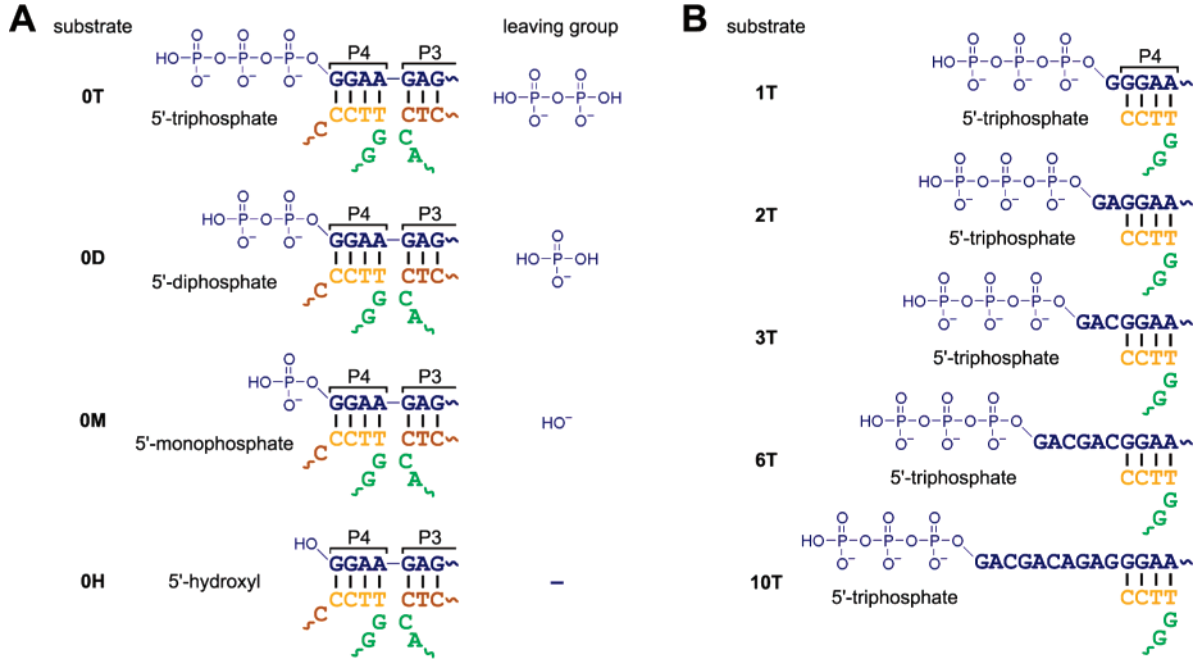

FIGURE 2: Right-hand (R) RNA substrates for testing the leaving group dependence of the 7S11 deoxyribozyme. For the nucleotide context, compare the illustrated sequence portions to paired regions P4 and P3 as marked in Figure 1A. (A) RNA substrates for which the leaving group was changed but zero extra nucleotides were added (hence the **0** designation). (B) RNA substrates with 1−10 nucleotides added at the 5′-end. The **T** (triphosphate = ppp) series is shown. For the **1** and **2** substrates, the **M** and **H** analogues were also examined (see the text).

prepared by 8−17 deoxyribozyme cleavage (*29*) of a 5′-lengthened precursor RNA transcript, which ensured that the 5′-terminus of **1H** and **2H** was a free 5′-hydroxyl group. The **1M** and **2M** substrates were prepared by 5′-monophosphorylation of **1H** and **2H** using ATP and PNK. The identities of all transcribed **1T**−**10T** substrates were confirmed by MALDI-MS, as were the identities of all RNA oligonucleotides prepared by solid-phase synthesis (data not shown).

Branch Formation. The ligation reactions were performed in the trimolecular assay format of Figure 1. The ^{32}P-radiolabeled left-hand RNA substrate L was the limiting reagent relative to the deoxyribozyme E and the right-hand substrate R. The L:E:R ratio was 1:5:15, with the concentration of E equal to ∼0.5 μM. The incubation was carried out in 50 mM CHES (pH 9.0), 150 mM NaCl, 2 mM KCl, and 40 mM $MgCl_2$ at 37 °C unless otherwise indicated. See our earlier reports for a detailed description of the methods of sample preparation and ligation analysis (*6*, *12*, *14*). For reactions of the **0T** and **0D** substrates (Figure 3), values of k_{obs} and final yield were obtained by fitting the yield versus time data directly to first-order kinetics; i.e., yield = $Y(1 - e^{-kt})$, where $k = k_{obs}$ and Y is the final yield. For reaction of **0M** (Figure 3), the k_{obs} was estimated by a linear fit to the initial data points.

Partial Alkaline Hydrolysis. For the assays of Figure 5, the **0T** and **1T** products were prepared by ligation in a 20 μL volume using 10 pmol of L substrate (5′-^{32}P-radiolabeled with [γ-^{32}P]ATP and PNK), with the L:E:R ratio equal to 1:3:6. The ligation products were purified by PAGE. The radiolabeled product (∼600 fmol) was incubated in 10 μL of 50 mM $NaHCO_3$ (pH 9.2) at 90 °C for 10 min.

RESULTS

Leaving Groups Other Than Pyrophosphate Allow 7S11-Catalyzed RNA Ligation. The 7S11 deoxyribozyme was previously identified through in vitro selection (*12*). As shown in Figure 1, 7S11 mediates reaction of a 2′-hydroxyl group on the left-hand (L) RNA substrate with the 5′-triphosphate on the right-hand (R) RNA substrate, forming 2′,5′-branched RNA (*12*, *14*). In this ligation reaction, the leaving group is pyrophosphate (PP_i; Figure 2A), which is not very basic and is therefore a relatively good leaving group. In our initial report (*12*), we also demonstrated that a 5′-adenylated substrate works well, with AMP instead of PP_i as the good leaving group. Here we examined the reactivity of a series of RNA substrates (Figure 2A) in which the nucleotide sequence of R was unchanged but the 5′-triphosphate (5′-ppp) was changed to either the 5′-diphosphate (5′-pp), 5′-monophosphate (5′-p), or 5′-hydroxyl group (5′-OH). To systematize the nomenclature, these R substrates are designated as **0T**, **0D**, **0M**, and **0H**, respectively. The **0** indicates that zero extra nucleotides have been added relative to the original R substrate, and the letter corresponds to the 5′-phosphorylation state. For the **0T** and **0D** substrates, the leaving groups are pyrophosphate (PP_i) and inorganic phosphate (P_i), respectively, each of which is a good leaving group (PP_i is better than P_i). In contrast, for the **0M** substrate, the leaving group is hydroxide anion (HO^-), which is a poor leaving group. Finally, for the **0H** substrate, no 5′-phosphorus atom is present, and therefore, no reaction at all should occur; this substrate serves as a negative control.

When the 5′-triphosphate (**0T**) of the right-hand RNA substrate was changed to 5′-diphosphate (**0D**), significant 7S11-mediated branch forming activity was maintained, although the k_{obs} was reduced by ∼50-fold (Figure 3A,B). A simple monophosphate anion (P_i) is therefore acceptable as the leaving group, in addition to PP_i and AMP. When the 5′-triphosphate was changed to a 5′-monophosphate (**0M**), branch formation was ∼10^3-fold slower than for **0T**, but

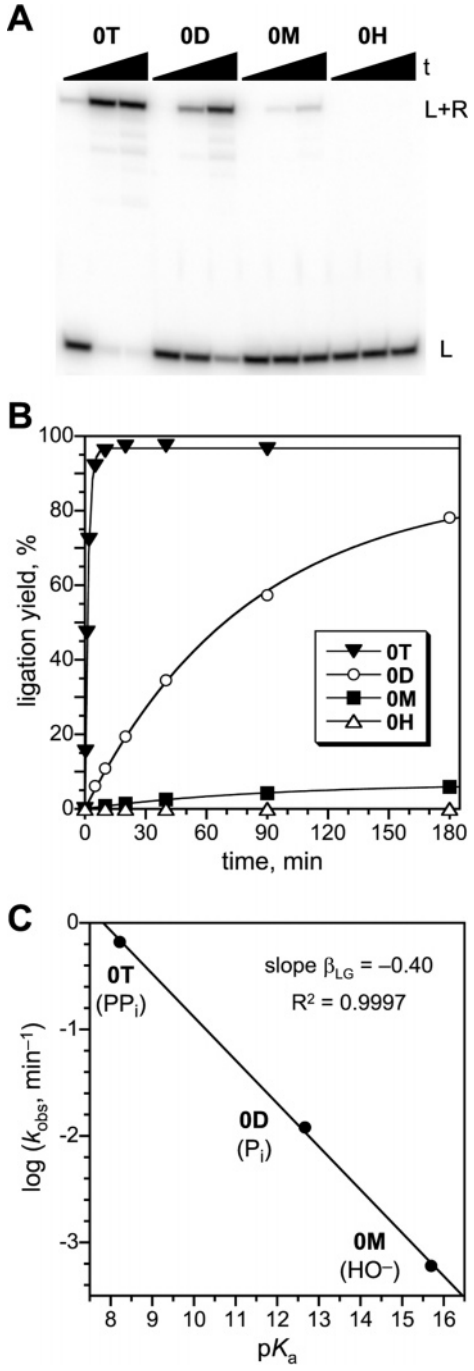

FIGURE 3: Effect of leaving group on 7S11-catalyzed branched RNA formation using the original-length R substrate. (A) Formation of branched RNA by 7S11 for RNA substrates with a 5′-triphosphate (**0T**), 5′-diphosphate (**0D**), 5′-monophosphate (**0M**), and 5′-hydroxyl group (**0H**). Time points were taken at 0, 20, and 180 min. L and R denote the RNA substrates as defined in Figure 1. (B) Kinetic plots. k_{obs} values were as follows: 0.66 min^{-1} for **0T**, 0.012 min^{-1} for **0D**, ~6×10^{-4} min^{-1} for **0M**, and no reaction observed for **0H** (<0.1%). Incubation was carried out in 50 mM CHES (pH 9.0), 150 mM NaCl, 2 mM KCl, and 40 mM $MgCl_2$ at 37 °C. Because of the method of synthesis (transcription using GDP; see Experimental Procedures), the **0D** sample has ~5% **0T** present. This is functionally irrelevant for the present experiment because any substantial contribution to the **0D** kinetic data from the **0T** component would be apparent as a fast second phase of the kinetic data. However, the data presented here for **0D** in panel B show no evidence of this fast component, indicating that the contribution from **0T** is negligible. (C) Brønsted plot for 7S11-catalyzed branch formation using the **0T**, **0D**, and **0M** substrates. Values of k_{obs} are from panel B; see the text for pK_a values.

detectable ligation activity still remained. In contrast to these observations, when the **0H** substrate that lacks any 5′-phosphorus atom was examined, no reaction whatsoever was observed, as expected. To provide additional evidence for the identities of the branched products using **0T** and **0M**, the ligation assays were performed using the alternative combination of substrates in which the right-hand substrate instead of the left-hand substrate was ^{32}P-radiolabeled. For both **0T** and **0M**, the product band was observed at the expected position in the gel, confirming the product assignments (see the Supporting Information).

The decreased k_{obs} values for **0D** and **0M** relative to that of **0T** may be compared with the expectations calculated from the basicities of the corresponding leaving groups. In a first-order analysis, the highest pK_a values for the relevant conjugate acids for **0T**, **0D**, and **0M** are 8.2 for pyrophosphoric acid, 12.7 for phosphoric acid, and 15.7 for water (*26*, *27*). When the experimental log(k_{obs}) values for **0T**, **0D**, and **0M** are plotted against these pK_a values, the points fall on a straight line with a Brønsted value (slope) β_{LG} of −0.40 ($R^2 = 0.9997$; Figure 3C).

Reactions with 5′-Extended RNA Substrates: Ligation Can Occur at Two Sites. We examined a second series of right-hand RNA substrates for which the 5′-termini were extended by one or more nucleotides (**1T**−**10T**, Figure 2B). For such substrates, there are two potential reaction sites: the α-phosphate of the 5′-terminal triphosphate and the internal original α-phosphate that immediately precedes the ...GGAA... sequence of P4. (For the nonextended **0T** substrate only, these two sites are identical; for all extended substrates, these two sites are distinct.) If the internal original α-phosphate is maintained as the reaction site for a 5′-extended RNA substrate, then the leaving group is the 3′-hydroxyl of a mononucleotide (**1T**) or oligonucleotide (**2T**−**10T**), which would mimic very closely the 5′-exon oligonucleotide leaving group of natural RNA splicing. The resulting branched RNA product is identical to that obtained with the original **0T** substrate, because the extra nucleotides of the 5′-extension depart with the leaving group. In contrast, if the 5′-triphosphate still reacts despite the extension because PP_i is a better leaving group than an oligonucleotide, then the resulting branched RNA product is larger than for **0T**, due to the extra nucleotides that are incorporated into the 2′-arm of the new branched junction. In this case, the spatial arrangement between nucleophile and electrophile as shown in Figure 1A is not maintained precisely.

The 5′-extended substrates were used to determine experimentally how the sites of reactivity depend on the leaving group stability and on the substrate length. For the **1T** substrate, the 5′-triphosphate is the only detectable reaction site (Figure 4). Because of the additional nucleotide, the branched product migrates slightly slower (i.e., higher) in the polyacrylamide gel. Partial alkaline hydrolysis unambiguously verified that the branch-site adenosine was maintained (Figure 5). For the **2T** substrate, both the 5′-triphosphate and the original α-phosphate are sites of nucleophilic attack with comparable rates, although both rates are considerably lower than for **0T** or **1T** (Figure 4). For the **3T**−**10T** substrates, the original α-phosphate is the only observed site of nucleophilic attack. As is the case for **2T**, the reaction rates and yields are low for **3T**−**10T**.

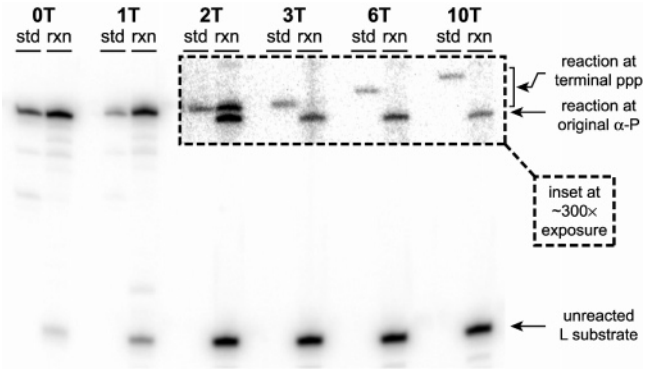

FIGURE 4: Effect of 5′-extension on 7S11-catalyzed RNA branch formation for a series of 5′-triphosphate substrates. The nucleotide sequences of the 5′-extensions are shown in Figure 2B. std indicates the branched RNA standard, prepared by an appropriate 7S11 deoxyribozyme with a shifted P4 region, that indicates the expected migration of the product from reaction at the 5′-triphosphate. rxn indicates the actual reaction product(s) observed for the particular 5′-extended substrate. Yields at the illustrated 180 min time points (corrected for background) were as follows: 99.5% for **0T**, 88.3% for **1T**, 0.36% (upper) and 0.48% (lower) for **2T**, 0.16% for **3T**, 0.17% for **6T**, and 0.082% for **10T**. The inset in the top right corner of the gel image is enhanced by ~300-fold so that the product bands are visible. The enhanced inset is shown directly on the gel image so that the positions of the various gel bands may be compared directly (see the Supporting Information for fully unenhanced and fully enhanced gel images). The k_{obs} for **1T** was approximately 50-fold lower than that for **0T** (data not shown), although their final yields are similar. The **10T** reaction product comigrates with the **0T** standard (data not shown).

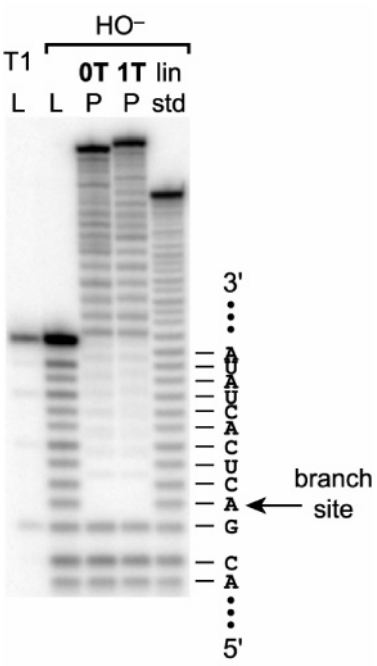

FIGURE 5: Partial alkaline hydrolysis reveals that the same branch-site adenosine 2′-hydroxyl of L attacks the 5′-triphosphate of both the **0T** and **1T** substrates. T1 indicates RNase T1 digestion (G-specific) for ladder calibration. HO^- indicates partial alkaline hydrolysis (50 mM $NaHCO_3$ at pH 9.2 and 90 °C for 10 min). L indicates the left-hand RNA substrate. P indicates the branched ligation product. lin std denotes the linear standard corresponding to the L + **0T** RNA sequences. The branch-site adenosine is revealed by the first missing band in the hydrolysis ladder. A similar assay could not be performed on the **2T**−**10T** branched products due to the relatively small amounts that were available (see Figure 4).

For the 5′-extended substrates that reacted entirely (**1T**) or partially (**2T**) at their 5′-terminal triphosphate, the monophosphate (**M**) and 5′-hydroxyl (**H**) versions of the same substrate sequences were tested (Figure 6A). In this one-nucleotide extension series, **1M** is observed to react at both its 5′-terminus and the original α-phosphate with comparable rates, with leaving groups of HO^- and GMP, respectively. In both cases, the rate is much lower than that for **1T**. As expected, no reaction occurs at the 5′-terminus of the **1H** substrate because there is no 5′-terminal phosphorus atom to attack, and therefore, reaction occurs at only the original α-phosphate, with guanosine (G) as the leaving group. In contrast, within the two-nucleotide extension series, no reaction occurs at the 5′-terminus of **2M** or **2H**; instead, reaction is observed at the original α-phosphate for both substrates, again with a very low rate. Taken together, these data demonstrate that a subtle balance of leaving group stabilization and 5′-extension length contributes to the site(s) of nucleophilic attack.

To confirm the product assignments for **1M**, we used an alternative combination of RNA substrates in which R instead of L was radiolabeled. When the original α-phosphate of **1M** is the site of nucleophilic attack, the branched RNA product should not be radioactive because ^{32}P will be within the GMP leaving group, leaving no radiolabel within the branched RNA itself. However, when the 5′-terminal phosphate of **1M** is the site of attack, the leaving group is HO^- and the branched RNA product should retain the radiolabel. As shown in Figure 6B, the observation of only the slower-migrating (upper) product band when **1M** itself is radiolabeled is consistent with these predictions.

With a longer R substrate, the same radiolabeling strategy that was used for **1M** above should be applicable, and the radiolabeled leaving group from attack at the original α-phosphate should in principle be detectable. For example, when **10T** itself is 5′-^{32}P-radiolabeled (technically, this substrate is **10M**), the displaced 10-nucleotide oligonucleotide leaving group and not the branched RNA product should contain the radiolabel. However, in practice, the identification of the small amount of the radiolabeled 10-nucleotide leaving group by PAGE was hindered by nonspecific degradation of R itself (data not shown).

A Binding Equilibrium Is Established for Certain 5′-Extended Substrates. For the 5′-extended substrate **10T**, the alternative **10T-alt-1** was tested (Figure 7). The important difference between **10T** and **10T-alt-1** is that the 5′-overhang of the latter begins with 5′-GGA. These three nucleotides have the potential to displace most of the substrate portion that composes 4-bp paired region P4, thus creating a 10-nucleotide bulge within the P4 duplex. When in the bulge structure, **10T-alt-1** should resemble **0T** in its reactivity, assuming that the bulge does not interfere. Experimentally, for **10T-alt-1** two distinct product bands are observed. The faster-migrating (lower) product is from reaction at the internal original α-phosphate, and the slower-migrating (higher) product is from reaction at the terminal 5′-triphosphate. In contrast, **10T** itself creates only the former product by reaction at the internal original α-phosphate (Figure 4), and **10T** cannot form the bulged **0T**-like structure that is accessible to **10T-alt-1**.

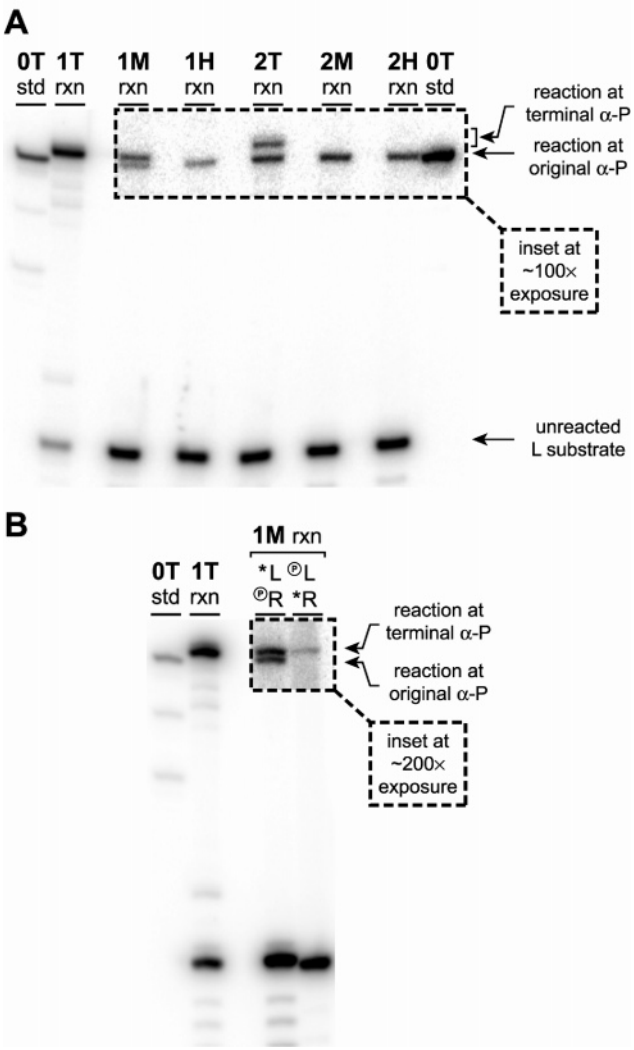

FIGURE 6: Effect of changing the leaving group for substrates with 5′-extensions of one or two nucleotides. The extension sequences are shown in Figure 2B. std indicates the branched RNA standard, prepared by an appropriate 7S11 deoxyribozyme, that indicates the expected position of the product from reaction at the activated 5′-triphosphate. rxn indicates the actual reaction product observed for the particular 5′-extended substrate. (A) Yields at the illustrated 180 min time points (corrected for background) were as follows: 91.8% for **1T**, 0.30% (upper) and 0.18% (lower) for **1M**, 0.21% for **1H**, 0.38% (upper) and 0.53% (lower) for **2T**, 0.49% for **2M**, and 0.39% for **2H**. The inset in the top right corner of the gel image is enhanced by ~100-fold so that the product bands are visible. The enhanced inset is shown directly on the gel image so that the positions of the various gel bands may be compared directly. See the Supporting Information for fully unenhanced and fully enhanced gel images. (B) Alternative radiolabeling combination for **1M**. Either the L or R substrate was 5′-^{32}P-radiolabeled as indicated (*). The circled P denotes 5′-monophosphorylation with nonradioactive ^{31}P.

To test directly the hypothesis that the overhang ⇆ bulge equilibrium of Figure 7 controls the site of reactivity, two additional substrates, **10T-alt-2** and **10T-alt-3**, were prepared. If the structural displacement for **10-alt-1** occurs as depicted, then **10T-alt-2** should react only at the internal original α-phosphate, whereas **10T-alt-3** should react only at the 5′-terminal triphosphate. Indeed, precisely these reactions were observed, which supports the binding equilibrium shown in Figure 7.

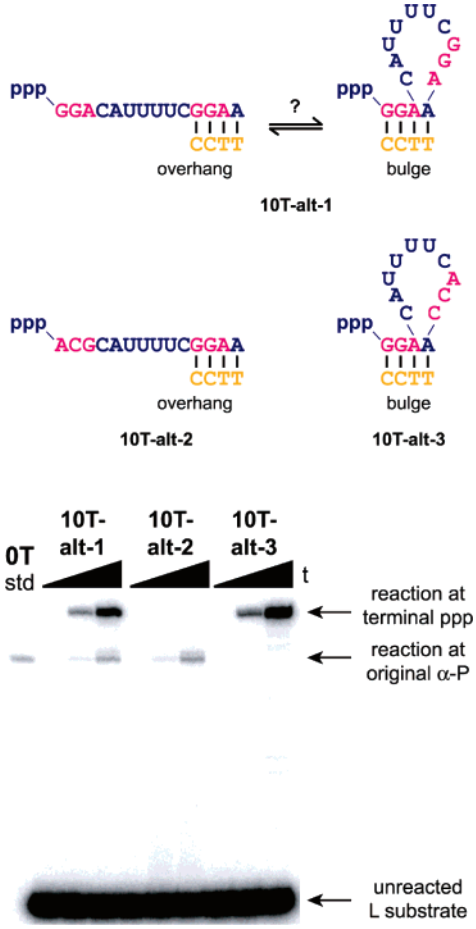

FIGURE 7: Alternative versions of the **10T** substrate, demonstrating that the reaction site is controlled by a two-state binding equilibrium. Time points are shown at 0, 20, and 180 min. Yields at 180 min (corrected for background) were 5.2% (upper) and 0.53% (lower) for **10T-alt-1**, 0.75% for **10T-alt-2**, and 12% for **10T-alt-3**.

DISCUSSION

Use of Relatively Poor Leaving Groups in Branched RNA Formation. The 7S11 deoxyribozyme that creates branched RNA was originally found to catalyze branch formation using a 5′-triphosphate RNA substrate, for which the leaving group is pyrophosphate (PP_i, Figure 1) (*12*). In the current study, we found that 7S11 also functions when the leaving group is monophosphate (P_i) or even the unactivated hydroxide anion (HO^-, Figure 3). Of course, HO^- is not normally considered a leaving group, so its observation in this role is somewhat surprising. The k_{obs} value for branch formation is diminished by ~50-fold when the leaving group is P_i versus PP_i (the **0D** vs **0T** substrates) and by $\sim 10^3$-fold when the leaving group is HO^- versus PP_i (the **0M** vs **0T** substrates). The linear Brønsted plot with a slope β_{LG} of −0.40 (Figure 3C) shows that the observed k_{obs} values are quantitatively consistent with the relative leaving group abilities of PP_i, P_i, and HO^-. The β_{LG} value itself indicates a substantial buildup of negative charge on the leaving group in the ligation transition state (*27*).

Because water and an oligonucleotide 3′-hydroxyl group have approximately equal pK_a values, one would expect that hydroxide and an oligonucleotide could function with nearly equal reactivities as leaving groups. However, to the extent that an alkoxide anion is somewhat more basic than hydroxide (i.e., that alcohols are slightly less acidic than

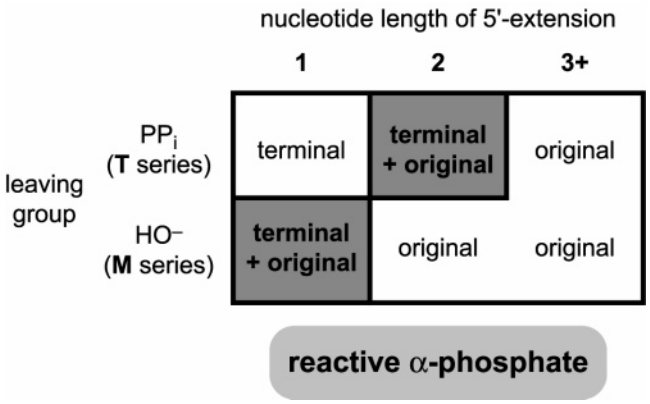

FIGURE 8: Summary of results with the 5′-triphosphate (**T**) and 5′-monophosphate (**M**) substrates for 5′-extended substrates. These substrates can potentially react at two sites: the α-phosphate at the 5′-terminus or the internal original α-phosphate (see Figure 1B). For substrates **1M** and **2T** (gray boxes), the balance between the competing reaction pathways is captured experimentally, because both possible reactions are observed in parallel.

water), an oligonucleotide should be a somewhat worse leaving group than hydroxide. Our experimental data are consistent with all of these expectations. In the 7S11-catalyzed ligation reaction, both hydroxide and an oligonucleotide can function as leaving groups, although the k_{obs} values are not identical. When the **0M** substrate reacts, hydroxide is the leaving group with a k_{obs} of $\sim 6 \times 10^{-4}$ min^{-1} (Figure 3). When the **1M** substrate reacts, a mononucleotide is the leaving group with a k_{obs} of $\sim 10^{-5}$ min^{-1} (Figure 6). Finally, when each of the 5′-extended substrates (**2T**, **3T**, **6T**, and **10T**) reacts, an oligonucleotide is the leaving group with a k_{obs} of $\sim 10^{-5}$ min^{-1} (Figure 4). Therefore, each of the 5′-extended substrates reacts ~1−2 orders of magnitude more slowly than **0M**, as expected for the differences in acidity between water and most alcohols (typically one to two pK_a units). The lower k_{obs} values for the 5′-extended substrates relative to that of **0M** may also reflect the fact that 7S11 was not selected to accept an oligonucleotide as the leaving group, and the use of such large leaving groups could inhibit the activity of the deoxyribozyme for steric reasons.

Capturing the Balance between Competing Reaction Pathways. When the 5′-terminus of an extended substrate retains the 5′-triphosphate (**1T**−**10T**, Figure 2B), a competition is established between two reaction sites (Figure 1B). The first reaction site is the α-phosphate of the 5′-terminal triphosphate, with PP_i as a good leaving group but not in its original position relative to the attacking 2′-hydroxyl nucleophile. The second site is the internal original α-phosphate, with an oligonucleotide as a poorer leaving group but at the original position with respect to the attacking nucleophile. Intriguingly, the balance between these competing pathways was precisely captured in two instances using the 5′-extended substrates (Figure 8). The **2T** substrate led to reaction at both sites with comparable efficiencies (Figure 4). In contrast, the shorter extended substrate **1T** reacted solely at its 5′-triphosphate, indicating that 7S11 tolerates a moderate structural perturbation while still retaining reactivity that involves the better PP_i leaving group. When the 5′-triphosphate of **1T** was replaced with the 5′-monophosphate of **1M**, again the balance between two pathways was observed, because both possible products were formed (Figure 6). In contrast to the observations with these shorter substrates, the longer extended substrates **3T**−**10T** reacted only at the internal original α-phosphate, even when a 5′-triphosphate was available farther away. Thus, a sufficiently large structural perturbation is not tolerated by 7S11; reactivity reverts entirely to the original α-phosphate site, even though an oligonucleotide instead of PP_i must be the leaving group.

The balance between competing reactions could also be modulated by strategically modifying the substrate sequence to favor one of two base pairing arrangements. The results with **10T-alt-1**−**10T-alt-3** are consistent with the simple binding equilibrium illustrated in Figure 7. Either the 5′-terminal triphosphate (**10T-alt-3**) or the internal original α-phosphate (**10T-alt-2**) is preferred as the reaction site, or both are utilized (**10T-alt-1**). The outcome is controlled by the sites that contribute to the P4 duplex on the basis of their sequence.

Extending the Parallel between Artificial and Natural Splicing Reactions. In our original report, we discerned a close similarity between 7S11-catalyzed branch formation and the first step of natural RNA splicing (*12*). This similarity was inferred primarily on the basis of a bulged branch-site adenosine nucleophile flanked by two duplex regions. Here we have strengthened the parallel between artificial and natural splicing by showing that the 7S11 branch-forming reaction can proceed with an oligonucleotide leaving group as a 5′-exon analogue. Of course, 7S11 is an artificial deoxyribozyme that is orders of magnitude less massive than the spliceosome, and 7S11 is approximately 10-fold smaller than most group II intron self-splicing RNAs (*28*). Despite these vast size differences and the fact that 7S11 was obtained in only a few weeks of in vitro selection, rather than millions of years of natural evolution, 7S11 shares structural and mechanistic similarities with the biological splicing catalysts. The extent to which other features of natural RNA splicing can be mimicked by artificial nucleic acid enzymes is an interesting question that is worthy of further investigation.

SUPPORTING INFORMATION AVAILABLE

Experiment with radiolabeled R for **0T** and **0M** and fully unenhanced and fully enhanced gel images from Figures 4 and 6A. This material is available free of charge via the Internet at http://pubs.acs.org.

REFERENCES

1. Gilbert, W. (1986) The RNA World, *Nature 319*, 618.
2. *The RNA World*, 2nd ed.; Gesteland, R. F., Cech, T. R., and Atkins, J. F., Eds.; Cold Spring Harbor Laboratory Press: Cold Spring Harbor, NY, 1999.
3. Doudna, J. A., and Cech, T. R. (2002) The chemical repertoire of natural ribozymes, *Nature 418*, 222−228.
4. Joyce, G. F. (2004) Directed Evolution of Nucleic Acid Enzymes, *Annu. Rev. Biochem. 73*, 791−836.
5. Silverman, S. K. (2004) Deoxyribozymes: DNA catalysts for bioorganic chemistry, *Org. Biomol. Chem. 2*, 2701−2706.
6. Flynn-Charlebois, A., Wang, Y., Prior, T. K., Rashid, I., Hoadley, K. A., Coppins, R. L., Wolf, A. C., and Silverman, S. K. (2003) Deoxyribozymes with 2′−5′ RNA Ligase Activity, *J. Am. Chem. Soc. 125*, 2444−2454.
7. Flynn-Charlebois, A., Prior, T. K., Hoadley, K. A., and Silverman, S. K. (2003) In Vitro Evolution of an RNA-Cleaving DNA Enzyme into an RNA Ligase Switches the Selectivity from 3′−5′ to 2′−5′, *J. Am. Chem. Soc. 125*, 5346−5350.

8. Ricca, B. L., Wolf, A. C., and Silverman, S. K. (2003) Optimization and Generality of a Small Deoxyribozyme that Ligates RNA, *J. Mol. Biol. 330*, 1015−1025.
9. Prior, T. K., Semlow, D. R., Flynn-Charlebois, A., Rashid, I., and Silverman, S. K. (2004) Structure−function correlations derived from faster variants of a RNA ligase deoxyribozyme, *Nucleic Acids Res. 32*, 1075−1082.
10. Wang, Y., and Silverman, S. K. (2003) Deoxyribozymes That Synthesize Branched and Lariat RNA, *J. Am. Chem. Soc. 125*, 6880−6881.
11. Wang, Y., and Silverman, S. K. (2003) Characterization of Deoxyribozymes That Synthesize Branched RNA, *Biochemistry 42*, 15252−15263.
12. Coppins, R. L., and Silverman, S. K. (2004) A DNA Enzyme that Mimics the First Step of RNA Splicing, *Nat. Struct. Mol. Biol. 11*, 270−274.
13. Coppins, R. L., and Silverman, S. K. (2004) Rational Modification of a Selection Strategy Leads to Deoxyribozymes that Create Native 3′−5′ RNA Linkages, *J. Am. Chem. Soc. 126*, 16426−16432.
14. Coppins, R. L., and Silverman, S. K. (2005) A Deoxyribozyme That Forms a Three-Helix-Junction Complex with Its RNA Substrates and Has General RNA Branch-Forming Activity, *J. Am. Chem. Soc. 127*, 2900−2907.
15. Wang, Y., and Silverman, S. K. (2005) Directing the Outcome of Deoxyribozyme Selections to Favor Native 3′−5′ RNA Ligation, *Biochemistry 44*, 3017−3023.
16. Semlow, D. R., and Silverman, S. K. (2005) Parallel Selections *in Vitro* Reveal a Preference for 2′−5′ RNA Ligation By Deoxyribozyme-Mediated Opening of a 2′,3′-Cyclic Phosphate, *J. Mol. Evol.* (in press).
17. Hoadley, K. A., Purtha, W. E., Wolf, A. C., Flynn-Charlebois, A., and Silverman, S. K. (2005) Zn^{2+}-Dependent Deoxyribozymes That Form Natural and Unnatural RNA Linkages, *Biochemistry 44*, 9217−9231.
18. Pratico, E. D., Wang, Y., and Silverman, S. K. (2005) A Deoxyribozyme That Synthesizes 2′,5′-Branched RNA with Any Branch-Site Nucleotide, *Nucleic Acids Res. 33*, 3503−3512.
19. Wang, Y., and Silverman, S. K. (2005) Efficient One-Step Synthesis of Biologically Related Lariat RNAs by a Deoxyribozyme, *Angew. Chem., Int. Ed. 44*, 5863−5866.
20. Silverman, S. K. (2004) Practical and general synthesis of 5′-adenylated RNA (5′-AppRNA), *RNA 10*, 731−746.
21. St. Maurice, M., and Bearne, S. L. (2004) Hydrophobic nature of the active site of mandelate racemase, *Biochemistry 43*, 2524−2532.
22. Rozan, L., Krysan, D. J., Rockwell, N. C., and Fuller, R. S. (2004) Plasticity of extended subsites facilitates divergent substrate recognition by Kex2 and furin, *J. Biol. Chem. 279*, 35656−35663.
23. Biou, V., and Cherfils, J. (2004) Structural principles for the multispecificity of small GTP-binding proteins, *Biochemistry 43*, 6833−6840.
24. Feng, H., Klutz, A. M., and Cao, W. (2005) Active site plasticity of endonuclease V from *Salmonella typhimurium*, *Biochemistry 44*, 675−683.
25. Milligan, J. F., Groebe, D. R., Witherell, G. W., and Uhlenbeck, O. C. (1987) Oligoribonucleotide synthesis using T7 RNA polymerase and synthetic DNA templates, *Nucleic Acids Res. 15*, 8783−8798.
26. *CRC Handbook of Chemistry and Physics*, 72nd ed.; Lide, D. R., Ed.; CRC Press: Boca Raton, FL, 1991.
27. Fersht, A. (1999) *Structure and Mechanism in Protein Science*, W. H. Freeman and Co., New York.
28. Michel, F., and Ferat, J. L. (1995) Structure and activities of group II introns, *Annu. Rev. Biochem. 64*, 435−461.
29. Santoro, S. W., and Joyce, G. F. (1997) A general-purpose RNA-cleaving DNA enzyme, *Proc. Natl. Acad. Sci. U.S.A. 94*, 4262−4266.

BI0507229